Electronic Supplementary Material (ESI) for Chemical Communications

Supplementary Information

$Na_2Ti_6O_{13}$: A Potential Anode for Grid-Storage Sodium-Ion Batteries

Ashish Rudola[1], Kuppan Saravanan[1], Devaraj Sappani[1], Hao Gong[2] and Palani Balaya[1,*]

Department of Mechanical Engineering[1], Department of Materials Science and Engineering[2], National University of Singapore, Singapore-117576

[*]*Email: mpepb@nus.edu.sg*

Experimental Information

$Na_2Ti_6O_{13}$ was synthesized by a soft-template method using sodium acetate and titanium isopropoxide as the sodium and titanium sources, respectively. 3.64g of cationic surfactant, CTAB (hexadecyl-trimethyl-ammonium bromide) was dissolved in a mixture containing 30 mL mili Q water and 90 mL ethanol. Appropriate molar ratio of the sodium and titanium sources were then added and stirred for 12 h. The solution was then dried using a rotor-evaporator. The obtained powder was then sintered in air at 800°C for 6 h. Powder X-ray diffraction (PXRD) patterns were recorded using a D2 Phaser Bruker X-ray diffractometer equipped with Cu Kα radiation. The accelerating voltage and current were 40 kV and 40 mA, respectively. A step size of 0.02° was used with 0.2 seconds per step. The morphology of the product was examined using field emission scanning electron microscope (FESEM; model JEOL JSM-7000F) operated at 15 kV and 20 mA. A JEOL JEM-2010 instrument was used for obtaining high-resolution transmission electron microscopy (HRTEM) images as well as selected-area electron diffraction (SAED) patterns. For TEM studies, the powder was dispersed in ethanol and sonicated, before being loaded on a Cu grid and dried.

For sodium storage studies without conductive additives, electrodes were fabricated with the active material and binder (Kynar 2801) in the weight ratio 90:10 using N-methyl pyrrolidone (NMP) as solvent. For the composite electrodes with conductive additives, the active material, Super P carbon black or graphite (Alfa Aesar), and binder were mixed in the weight ratio 70:20:10 using NMP as solvent. The obtained slurry was coated uniformly on a 15 µm thick etched aluminium foil (Shenzhen Vanlead Technology) using a doctor blade and dried at 110°C under vacuum for 12 h. The dried slurry was pressed using a twin roller of 37 psi. The active material loading was around 1.0 mg/cm^2 (in practice, thicker loadings of 2.6 mg/cm^2 also resulted in similar performance). Sodium metal foil, 1 M $NaClO_4$ in ethylene carbonate (EC) (Alfa Aesar) and propylene carbonate (PC) (1:1 volume ratio) (Merck) and Whatman Glass Microfibre Filter (Grade GF/F) were used as counter electrode, electrolyte and separator, respectively, to assemble coin-type cells (size 2016) in an argon filled glove box (MBraun, Germany). The sodium metal rods (Merck), immersed in kerosene, were wiped clean, cut into slices, rolled into the desired thickness and finally cut into circular disks. All cells contained a stainless steel spring between the sodium disk and the coin cell container to establish better contact. Charge–discharge cycling at a constant current mode was carried out using a computer controlled Arbin battery tester (Model, BT2000, USA) and cyclic voltammetry (CV) studies were carried out at room temperature using a computer controlled VMP3 (Bio-logic, France) in the voltage window 0.5 – 2.5V. For the *ex-situ* XRD studies of the cycled pure electrodes (without any carbon black) at different voltages, the electrode was charged/discharged at a rate of C/5. The discharged material was found to be unstable in air. This instability could be conveniently followed from the colour change of the electrodes- the fully discharged electrode was black in colour. It took approximately 15 – 30 minutes in ambient air for the discharged electrode to start to change its colour to white. Hence, for the *ex-situ* studies, the electrodes were sealed in Ar filled containers in glove box and opened just prior to measurement. The total measurement time was 5 minutes. The discharged electrode was hence, black in colour even after recording the XRD spectrum. Regardless of such air exposure time (after the electrodes were opened prior to PXRD measurement until the data were collected), it may be noted that there is no way to know by ex-situ XRD if there has been any structural change of the cycled electrode materials, since their XRD patterns have shown very small differences with respect to pristine material. For the variable temperature thermal XRD studies, the spectrum was obtained in vacuum. Rietveld refinement was performed using TOPAS 3.0 software, while the calculations to determine the lattice parameters at the various states of charge and discharge for the *ex-situ* XRD experiments were carried out using Prozski software, by following the shift in the 200, -201, 110, 310, 402 and 020 peaks. Thermogravimmetric analysis (TGA) was performed on a sodiated $Na_2Ti_6O_{13}$ powder of weight around 2mg in an alumina pan under nitrogen atmosphere with a ramp rate of 10°C/min.

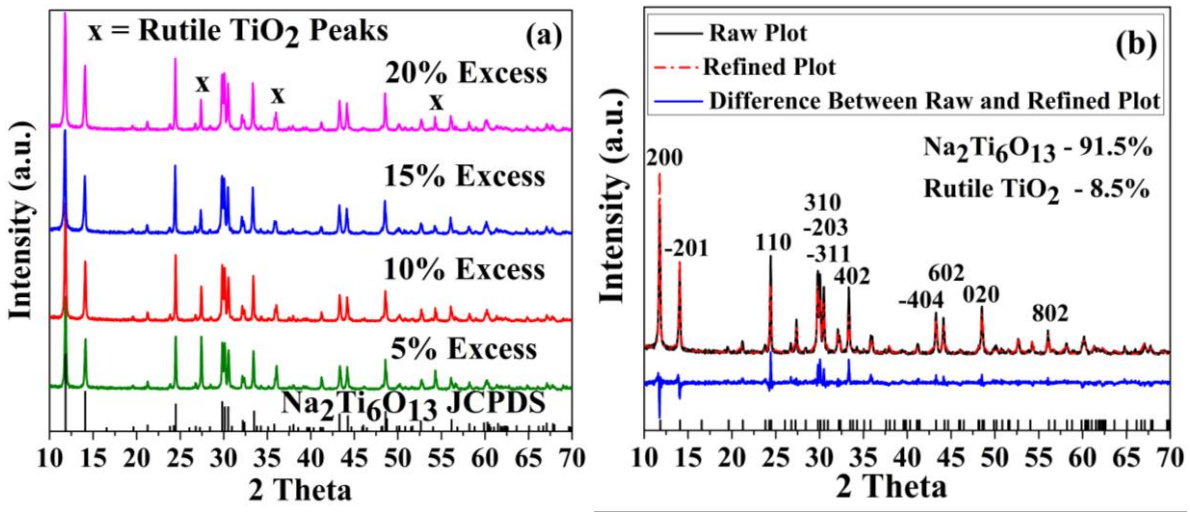

Fig. S1 (a) PXRD patterns of the as-synthesized $Na_2Ti_6O_{13}$ powders, as a function of the excess of sodium to titanium stoichiometric molar ratio. (b) Rietveld refinement of the as-prepared sample with 15% molar excess of the sodium source, with respect to the titanium source. A consideration of preferential orientation during refinement did not improve the fitting.

Table S1 Phase purity of the as-prepared $Na_2Ti_6O_{13}$ samples for different molar ratio of the Na and Ti sources, as determined from Rietveld refinement of PXRD data

Samples with different Na:Ti ratio	**Molar Stoichiometry (Na:Ti)**	**$Na_2Ti_6O_{13}$ Phase (%)**	**Rutile TiO_2 (%)**
5% Excess	1.05 : 3	81.5	18.5
10% Excess	1.10 : 3	88.6	11.4
15% Excess	1.15 : 3	91.5	8.5
20% Excess	1.20 : 3	90.5	9.5

Table S2 Lattice parameters obtained for the as-prepared $Na_2Ti_6O_{13}$ samples, as determined from Rietveld refinement. The errors were calculated using Bragg's law and the instrument resolution (0.01°)

Space Group	**a (Å)**	**b (Å)**	**c (Å)**	**β (°)**	**Volume (Å^3)**	**R-Bragg**	**R_{wp}**	**χ^2**
C2/*m*	15.094± 0.009	3.7434± 0.0007	9.168± 0.004	99.016± 0.015	511.6± 0.7	8.060	17.810	1.560

Table S3 Refined crystallographic data for the as-prepared $Na_2Ti_6O_{13}$ samples, as determined from Rietveld refinement. All values of x, y and z atomic positions have errors confined to the last digit.

Site	**Wyckoff**	**x**	**y**	**z**	**Atom**	Occ	$\mathbf{B_{iso}}$
Na1	4*i*	0.4540	0.0000	0.2508	Na+1	1	1
Ti1	4*i*	0.1137	0.0000	0.0895	Ti+4	1	1
Ti2	4*i*	0.1705	0.0000	0.4332	Ti+4	1	1
Ti3	4*i*	0.2287	0.0000	0.7726	Ti+4	1	1
O1	2*a*	0.0000	0.0000	0.0000	O-2	1	1
O2	4*i*	0.2280	0.0000	0.2470	O-2	1	1
O3	4*i*	0.0710	0.0000	0.2910	O-2	1	1
O4	4*i*	0.2820	0.0000	0.5740	O-2	1	1
O5	4*i*	0.1240	0.0000	0.6170	O-2	1	1
O6	4*i*	0.3580	0.0000	0.8840	O-2	1	1
O7	4*i*	0.1670	0.0000	0.9270	O-2	1	1

Table S4 Refined crystallographic data for the rutile TiO_2 impurity in the as-prepared $Na_2Ti_6O_{13}$ samples, as determined from Rietveld refinement. All values of x, y and z atomic positions have errors confined to the last digit.

Site	**Wyckoff**	**x**	**y**	**z**	**Atom**	Occ	$\mathbf{B_{iso}}$
Ti1	2*a*	0.0000	0.0000	0.0000	Ti+4	1	1
O1	4*f*	0.3057	0.3057	0.0000	O-2	1	1

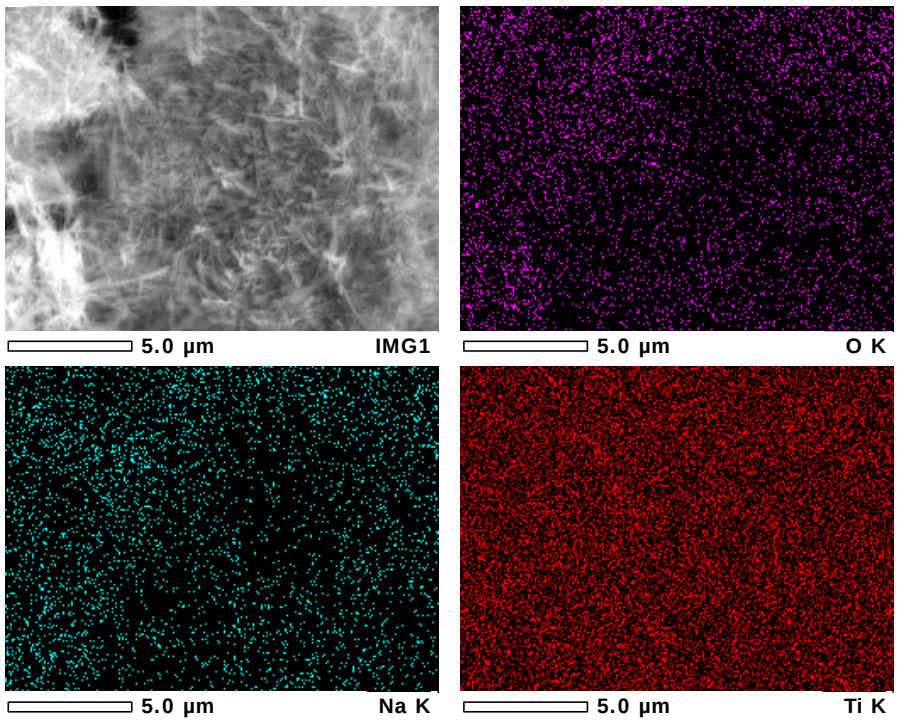

Fig. S2 Energy Dispersive X-ray Spectroscopy spectra of the as-prepared $Na_2Ti_6O_{13}$ nanorods, clearly demonstrating a uniform distribution of Na, Ti and O throughout the sample.

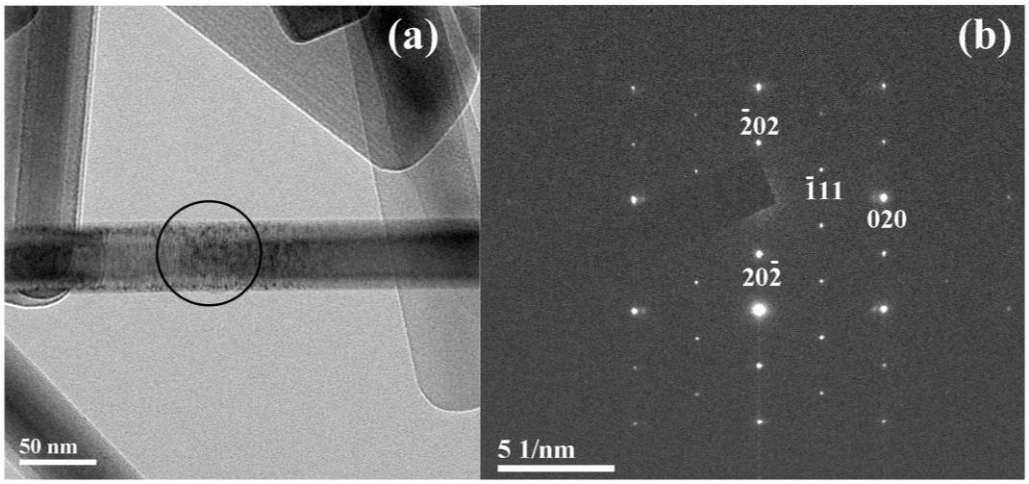

Fig. S3 (a) TEM image of an isolated nanorod with the corresponding SAED pattern depicted in (b), showing the single-crystalline nature of the rod. The indexed spots highlight that the rod grows preferentially along [010], the *b*-axis. The SAED pattern was recorded along the [101] zone axis.

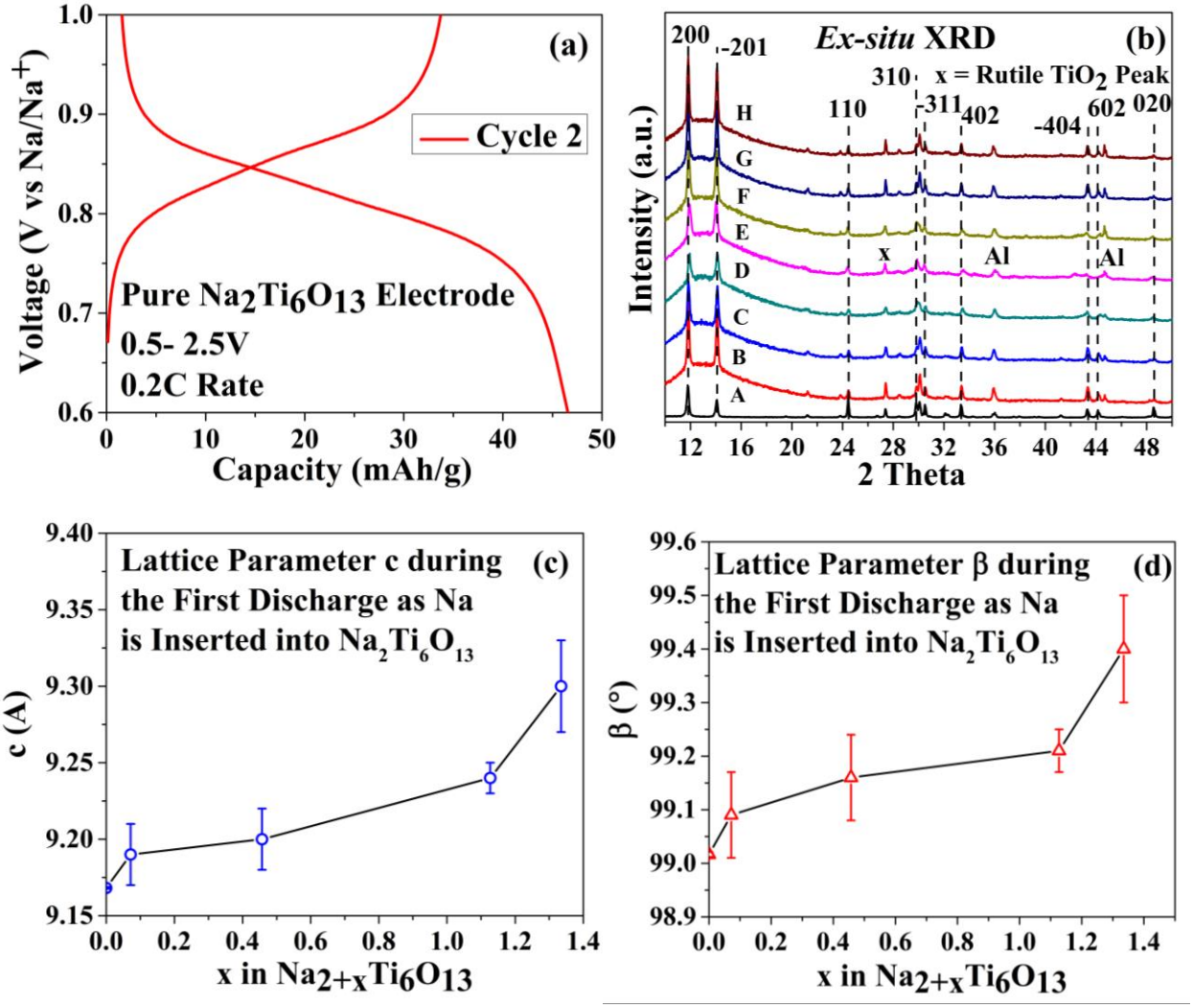

Fig. S4 (a) Cycle 2 of a pure $Na_2Ti_6O_{13}$ electrode at a C/5 rate is shown for illustration. The clear sloping nature of the plateau is seen, when the y-axis scale is changed to 0.6-1.0V, instead of the usual 0.5-2.5V. This sloping plateau indicates a solid-solution nature of sodium storage. This was supported by (b) which depicts the *ex-situ* XRD of the pure $Na_2Ti_6O_{13}$ electrode at various points indicated by points in Fig. 1c of the main text. The entire 10 – 50 ° 2 Theta range is depicted. No new peaks were seen at any states of charge/discharge. "Al" represents the peaks contributed from the Al current collector substrate. The continuous change in the lattice parameters c and β, with increasing sodium insertion into $Na_2Ti_6O_{13}$, is depicted in (c) and (d), respectively.

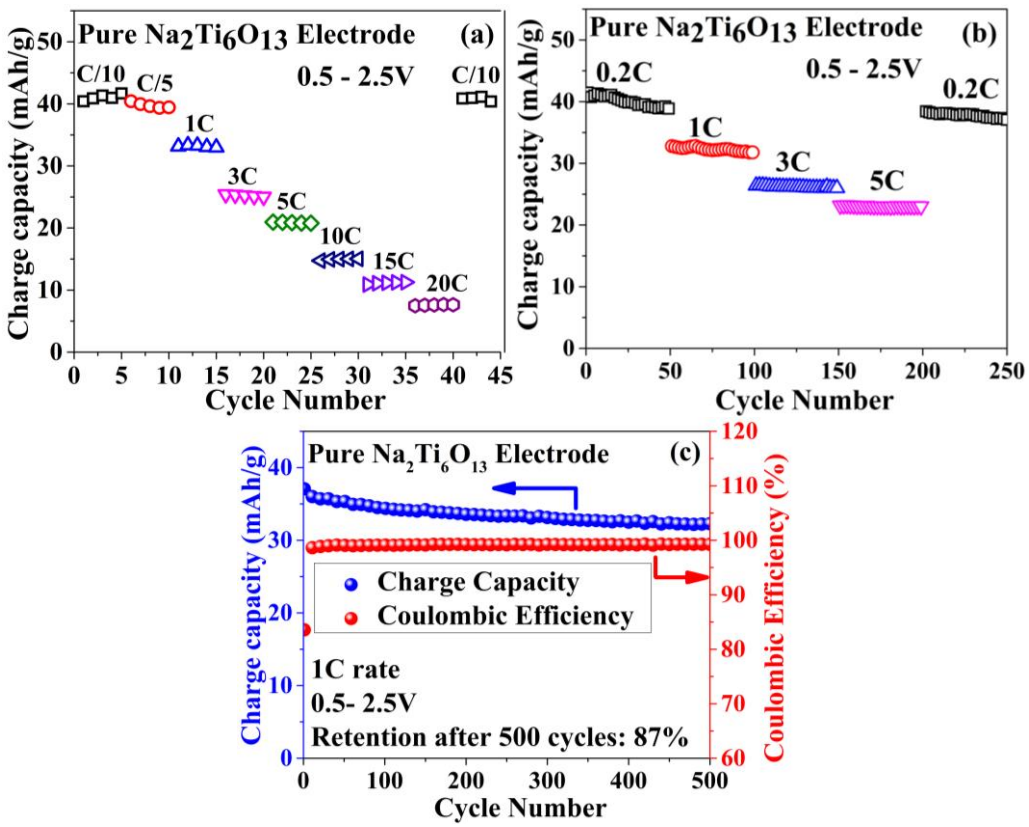

Fig. S5 Rate performance of a pure $Na_2Ti_6O_{13}$ electrode from (a) C/10 to 20C rate and (b) Rate performance of a pure $Na_2Ti_6O_{13}$ electrode over 50 cycles each at C/5, 1C, 3C, 5C and back to C/5. Even at low C-rates, where more than 80% of the theoretical capacity was obtained, the cycling was stable, indicative of the excellent reversibility of this material towards sodium intercalation/de-intercalation. (c) 500 cycles of a pure $Na_2Ti_6O_{13}$ electrode showing the charge capacity and coulombic efficiency at 1C rate.

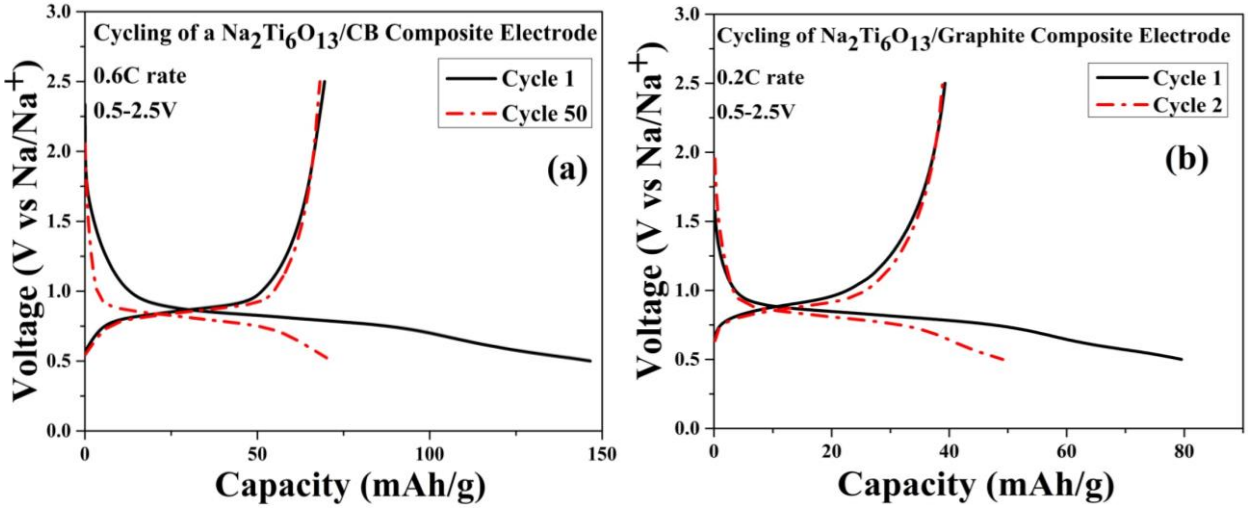

Fig. S6 (a) Cycles 1 and 50 of a $Na_2Ti_6O_{13}$/CB composite electrode, depicting the huge first discharge capacity. (b) Cycles 1 and 2 of a $Na_2Ti_6O_{13}$/graphite composite electrode, illustrating that the irreversible capacity loss increases by only a small amount when graphite is used, as opposed to use of CB, with respect to a pure $Na_2Ti_6O_{13}$ electrode (see Fig. 1c in the main text).

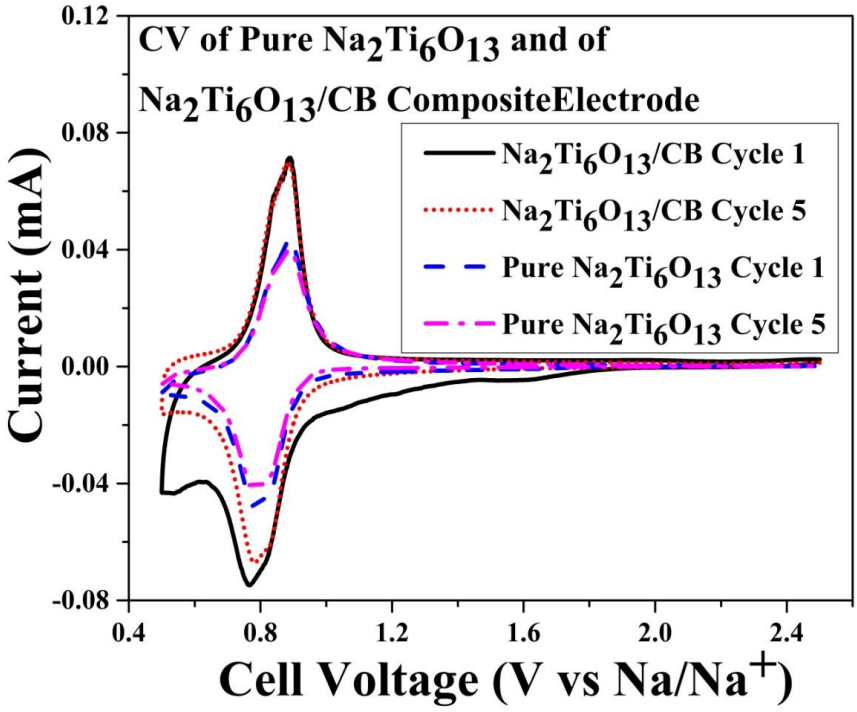

Fig. S7 Cyclic voltammograms of the first and the fifth cycles of a pure $Na_2Ti_6O_{13}$ and a $Na_2Ti_6O_{13}$/CB composite electrode at a 0.05 mV/s scan rate. The first reduction (sodium intercalation) of the composite electrode displayed a big, broad peak around 0.55 V, which disappeared in subsequent cycles, consistent with the disappearance of the tail of the discharge plateau in the subsequent galvanostatic cycles (Fig. S6a). Furthermore, this peak was not present in the first cycle CV curve of the pure $Na_2Ti_6O_{13}$ electrode (refer to Fig. S7). Hence, this big irreversibility can be attributed to the carbon black additive. Due to the facts that the fifth cycle of the $Na_2Ti_6O_{13}$/CB composite electrode displayed three times the current between 0.7 – 0.5 V in the reduction process as compared to the fifth cycle reduction of a pure $Na_2Ti_6O_{13}$ electrode and that both electrodes had similar subsequent oxidation curves, it can be stated that the carbon black additives also take part in the sodium storage in this composite electrode

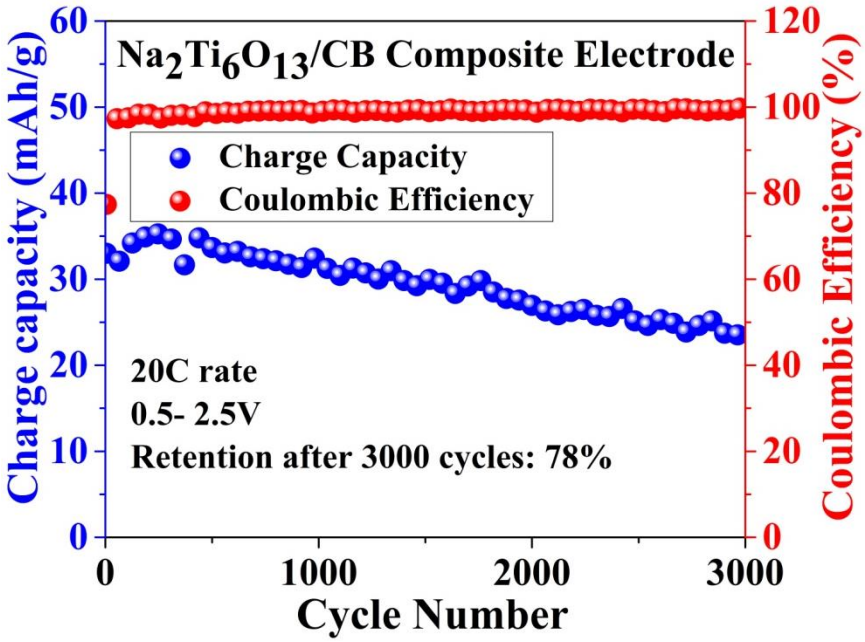

Fig. S8 3,000 cycles of a $Na_2Ti_6O_{13}$/CB composite electrode showing the charge capacity and coulombic efficiency at 20C rate.

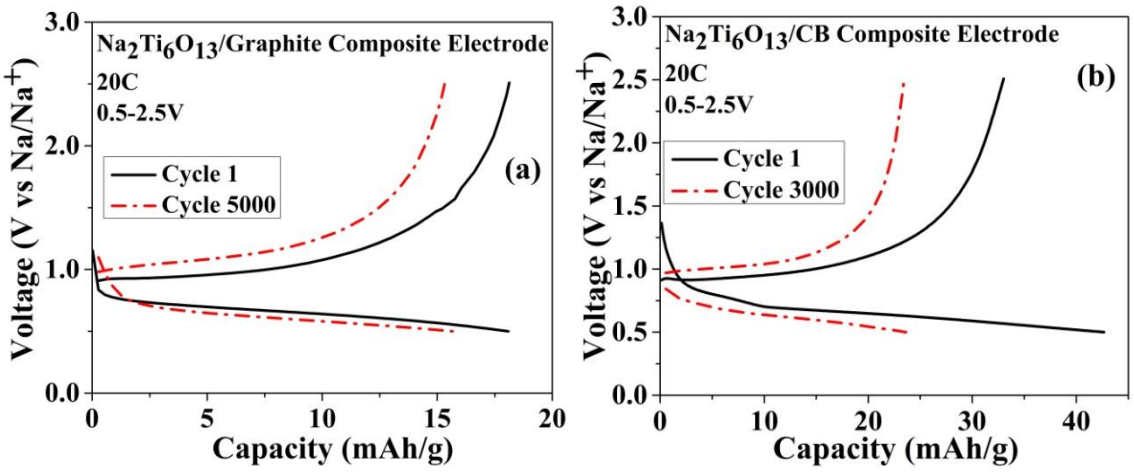

Fig. S9 (a) Cycles 1 and 5,000 of a $Na_2Ti_6O_{13}$/graphite composite electrode and (b) Cycles 1 and 3,000 of a $Na_2Ti_6O_{13}$/CB composite electrode at a fast 20C (3 min. charge/discharge) rate. The plateau is clearly visible even in this range, suggesting robustness of the electrodes upon long term cycling at high rates.

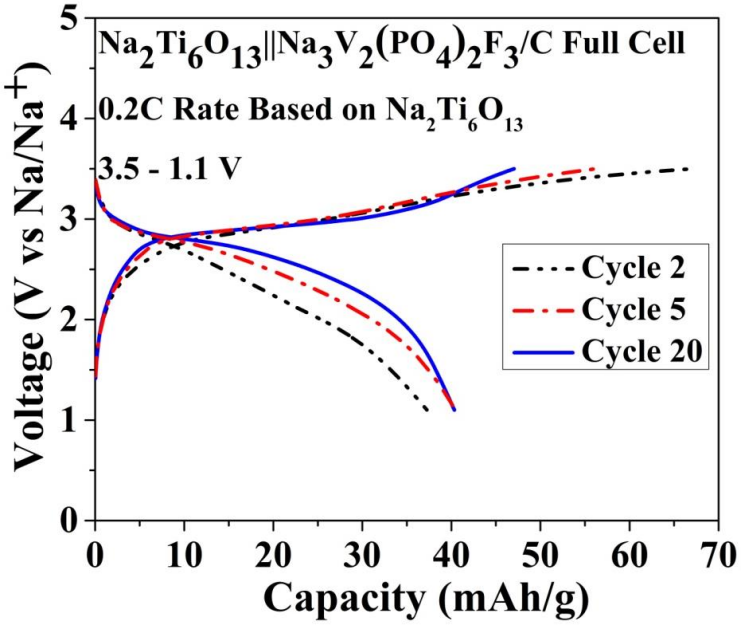

Fig. S10 A pure $Na_2Ti_6O_{13}$‖ $Na_3V_2(PO_4)_2F_3$/C full cell cycled at a C/5 rate, between 3.5 – 1.1 V. A capacity of 41 mAh/g was obtained, and found to be stable, after 20 cycles. The capacity is displayed with respect to the anode weight, as excess cathode was utilized in this full cell. The electrolyte used was 1M $NaClO_4$ in EC:PC (1:1 volume ratio)

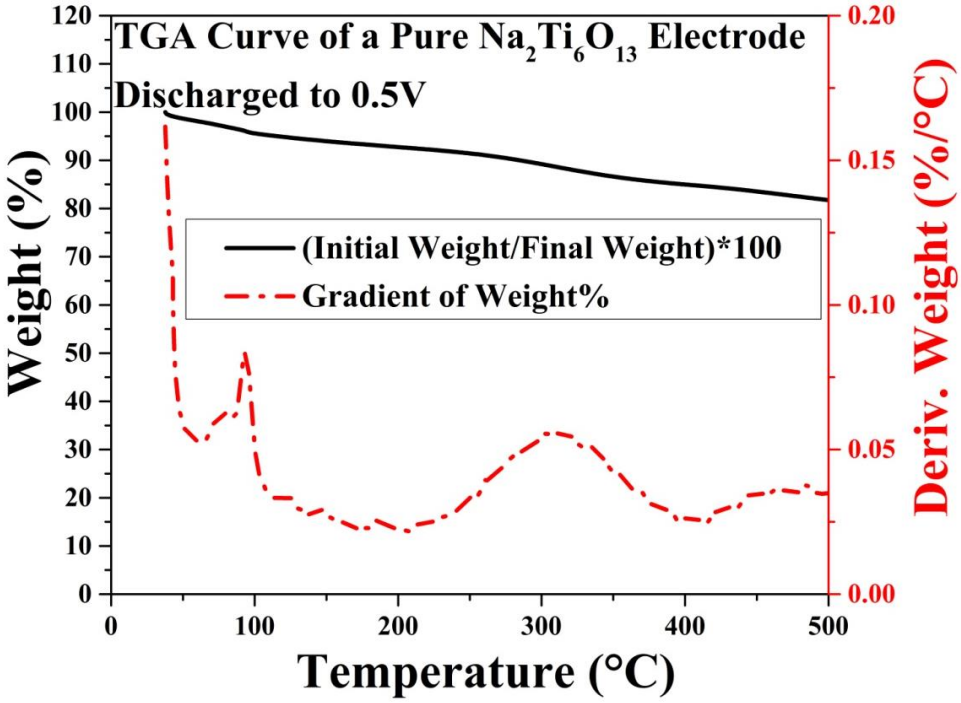

Fig. S11 TGA curve of a pure $Na_2Ti_6O_{13}$ electrode discharged to 0.5V showing the loss of weight and its gradient. Majority of the weight loss takes place close to 100 and 310 °C, which can be attributed to surface-adsorbed moisture and melting of residual $NaClO_4$ salt, respectively. Hence, the sodiated $Na_2Ti_6O_{13}$ material does not undergo much weight loss till 500 °C.